An Error-Prone Viral DNA Ligase†

Brandon J. Lamarche,‡ Alexander K. Showalter,‡ and Ming-Daw Tsai*,‡,§

Departments of Chemistry and Biochemistry, The Biophysics Program, and The Ohio State Biochemistry Program, The Ohio State University, Columbus, Ohio 43210, and Genomics Research Center, Academia Sinica, Taiwan

Received October 27, 2004; Revised Manuscript Received March 31, 2005

ABSTRACT: Our recent demonstration that DNA polymerase X (Pol X), the DNA repair polymerase encoded by the African swine fever virus (ASFV), is extremely error prone during single-nucleotide gap filling led us to hypothesize that it might contribute to genetic variability in ASFV. For the infidelity of Pol X to be relevant, however, the DNA ligase working downstream of it would need to be capable of sealing nicks containing 3′-OH mismatches. We therefore examined the nick ligation capabilities of the ASFV-encoded DNA ligase and here report the first complete 3′ fidelity analysis, employing catalytic parameters, for any DNA ligase. The catalytic efficiency of nick sealing by both ASFV DNA ligase and bacteriophage T4 DNA ligase was determined in the steady state for substrates containing all 16 possible matched and mismatched base pair combinations at the 3′ side of a nick. Our results indicate that ASFV DNA ligase is the lowest-fidelity DNA ligase ever reported, capable of ligating a 3′ C:T mismatched nick (where C and T are the templating and nascent nucleotides, respectively) more efficiently than nicks containing Watson−Crick base pairs. Comparison of the mismatch specificity of Pol X with that of ASFV DNA ligase suggests that the latter may have evolved toward low fidelity for the purpose of generating the broadest possible spectrum of sealed mismatches. These findings are discussed in light of the genetic and antigenic variability observed among some ASFV isolates. Two novel assays for determining the concentration of active DNA ligase are also reported.

ASFV[1] is a large [168−189 kb (*1*)] double-stranded DNA virus that infects domestic pigs in Africa, the Iberian Peninsula, and the Caribbean (*2*, *3*). The virus principally targets macrophage cells (*3*) where it displays a distinct phase of DNA synthesis in the cytoplasm prior to viron assembly (*4*, *5*). Antigenic differences among field isolates suggest that ASFV exists as a diverse population of serotypes in some regions of Africa (*6*). Additionally, restriction fragment length polymorphisms, in the absence of major genome rearrangements, are consistent with genetic diversity in ASFV arising from point mutations or small insertions and/or deletions (*7*).

Consistent with its intracellular location, ASFV encodes its own replicative DNA polymerase and three base excision repair (BER) enzymes: a putative class II AP endonuclease (APE), the repair polymerase Pol X, and an ATP-dependent DNA ligase (*8*). We have demonstrated Pol X to be structurally and functionally unique (*9*, *10*). At just 174 amino acids, Pol X is the smallest polymerase identified to date, lacking the N-terminal domain (responsible for DNA binding) that is present in its eukaryotic homologue polymerase β (Pol β) (*10*, *11*). When filling single-nucleotide gaps, Pol X is error-prone and, in particular, catalyzes the formation of G:G mismatches with an efficiency comparable to that of the correct, Watson−Crick G:C base pair (*9*). This led us to hypothesize a potential "mutator" role for this enzyme (*9*). However, for such an activity to be physiologically relevant, a DNA ligase of low fidelity, capable of sealing nicks at 3′ mismatched base pairs, would be requisite; if refractory to ligation, mismatched nicks would ultimately block genome replication and be lethal to the virus. A cursory, qualitative analysis indicated that ASFV DNA ligase can indeed ligate a 3′ G:G mismatch relatively efficiently (*10*).

In this paper, we first demonstrate two novel assays for determining the concentration of active DNA ligase. These techniques enable quantitation of both the total active enzyme concentration and the concentration of active enzyme in its two principle forms [with and without the covalently bound cofactor adenosine monophosphate (AMP)]. Subsequently, we report a complete 3′ fidelity analysis of nick sealing by ASFV DNA ligase. Since it was previously demonstrated to efficiently seal a 3′ G:T mismatched nick (*12*), T4 DNA ligase was also assayed to serve as a reference. Nick sealing capabilities were examined in the steady state using substrates containing all 16 possible 3′-OH base pair combinations. Our data indicate that ASFV DNA ligase is more tolerant of 3′-

† This work was supported by NIH Grant GM43268. B.J.L. was supported in part by a predoctoral NIH CBIP fellowship (2T32 GM08512).

* To whom correspondence should be addressed at the Department of Chemistry. Phone: (614) 292-3080. Fax: (614) 292-1532. E-mail: tsai@chemistry.ohio-state.edu.

‡ Department of Chemistry, The Ohio State University.

§ Department of Biochemistry, The Biophysics Program, and The Ohio State Biochemistry Program, The Ohio State University, and Academia Sinica.

[1] Abbreviations: Pol, DNA polymerase; ASFV, African swine fever virus; BER, base excision repair; AP, apurinic/apyrimidinic (abasic); APE, AP endonuclease; BSA, bovine serum albumin; AEBSF, 4-(2-aminoethyl)benzenesulfonyl fluoride; PMSF, phenylmethanesulfonyl fluoride; PNK, polynucleotide kinase; adenylyl, adenosine monophosphate (AMP); 5′-dRP, 5′-deoxyribose phosphate; SHM, somatic hypermutation.

10.1021/bi047706g CCC: $30.25
Published on Web 05/18/2005

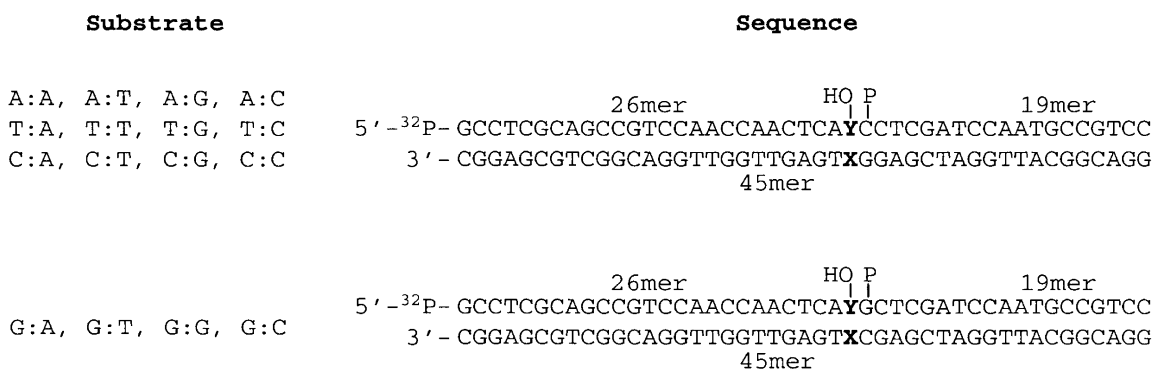

FIGURE 1: Nicked DNA substrates. Substrates are named according to the base pair which is 3′ (upstream) with respect to the nick. This base pair is described as X:Y, where X denotes the templating nucleotide and Y represents the nucleotide that would have been incorporated by a polymerase in the preceding gap-filling step. OH is the 3′-hydroxyl, and P is the 5′-phosphate.

OH mismatches than any DNA ligase yet reported. A comparison of the mismatch specificities of ASFV DNA ligase and Pol X provides some insight into the selective pressure that may have driven the coevolution of these two enzymes. These findings are discussed in light of the genetic diversity observed among some ASFV isolates.

EXPERIMENTAL PROCEDURES

Materials. TOP10 cells and the pBAD/HisB plasmid were from Invitrogen. Complete, EDTA-free protease inhibitor cocktail tablets and bovine serum albumin (BSA) were from Roche. 4-(2-Aminoethyl)benzenesulfonyl fluoride (AEBSF) was from BioShop. Phenylmethanesulfonyl fluoride (PMSF) and Tween 20 were from Sigma. L-Arabinose was from Aldrich. Hydroxyapatite was from Bio-Rad, and P-11 was from Whatman. Amicon centrifugal filter devices were from Millipore. 2′-Deoxy-3′-aminocytidine triphosphate and the 5′-adenylylated 19mer oligonucleotide were from TriLink. All other oligonucleotides were from Integrated DNA Technologies (IDT). T4 DNA ligase and T4 polynucleotide kinase (PNK) were from New England Biolabs. Sep-Pak C18 columns were from Waters. ATP and Microspin G-25 columns were from Amersham Biosciences. Materials and reagents not listed here were of standard molecular biology grade.

Cloning, Protein Expression, and Protein Purification. The ASFV DNA ligase gene was subcloned from pET 17b-ASFV ligase (*10*) into the NcoI and KpnI sites of pBAD/HisB, which contains an arabinose inducible promoter. This construct does not include the N-terminal His tag. Use of the NcoI site resulted in the conservative leucine to valine mutation at amino acid 2. With this plasmid, optimal yields of ASFV DNA ligase are obtained in TOP10 cells (which do not metabolize arabinose). After the cells had reached mid-log phase in SOB medium at 37 °C, the temperature was decreased to 30 °C, L-arabinose added to a concentration of 0.13% (w/v), and shaking continued for 6 h before the cells were harvested by centrifugation. Protein purification was carried out at 4 °C in a buffer consisting of 50 mM Tris-HCl, 400 mM KCl, 10% glycerol, 1 mM EDTA (pH 8.0 at 4 °C), and 10 mM DTT. Cells were lysed by sonication in this buffer supplemented with 100 μM PMSF, 100 μM AEBSF, and complete protease inhibitor cocktail according to the manufacturer's protocol. After cellular debris had been pelleted, the clarified lysate was applied to a DEAE column [8 cm × 5 cm (inside diameter)] that had been equilibrated with the same buffer. The flow through, including 600 mL of wash (using the same buffer), was applied to a P-11 column that was then washed with 1 L of the same buffer. Elution was carried out in purification buffer using a linear KCl gradient (from 0.4 to 1.4 M; 350 mL total volume) at a flow rate of ~0.8 mL/min, collecting 5.6 mL fractions. ASFV DNA ligase-containing fractions (which eluted between 500 and 800 mM KCl) were pooled, concentrated in an Amicon centrifugal filter device (10 kDa molecular mass limit), and loaded onto an S-100 column [200 cm × 3 cm (inside diameter)] equilibrated with 150 mM KCl purification buffer. ASFV ligase eluted from this column in the void volume along with a high-molecular mass contaminant. We found that by rerunning the sample on an S-200 column in the presence of 4% Tween 20 we could resolve the two proteins. Ligase-containing S-200 eluate was pooled and dialyzed into 10 mM sodium phosphate, 10% glycerol, 50 μM EDTA (pH 7.3 at 4 °C), 10 mM DTT, and 0.5% Tween 20 before being loaded onto a hydroxyapatite column (1.2 cm inside diameter; bed volume of ~10 mL) that had been equilibrated with the same buffer. For washing and elution, a step gradient was employed, consisting of 20, 40, 80, 160, and 320 mM sodium phosphate. Tween 20 was excluded from the latter two steps. ASFV DNA ligase eluted, at >95% purity, late in the 320 mM step. Ligase-containing fractions were pooled and dialyzed against the following buffer: 50 mM Tris-borate, 100 mM KCl, 15% glycerol, and 10 mM DTT (pH 8.0 at 4 °C). After concentration, the sample was supplemented with glycerol to a final concentration of 50% (v/v), flash-frozen in liquid N_2, and stored at −80 °C. Subsequently, working aliquots were kept at −20 °C.

T4 DNA ligase from New England Biolabs was used without further purification. Rat Pol β was expressed and purified as described by Dunlap and Tsai (*13*).

Preparation of DNA Substrates. Oligonucleotides were purified by denaturing polyacrylamide electrophoresis under standard conditions. After gel extraction, oligos were desalted on Sep-Pak C18 columns, dried in a speed-vac, and resuspended in TE buffer [10 mM Tris-HCl and 1 mM EDTA (pH 7.5)]. Concentrations were determined by the UV absorbance at 260 nm using extinction coefficients calculated by the oligo analyzer tool on IDT's Web site.

The appropriate oligonucleotides were labeled using T4 polynucleotide kinase (PNK) and [γ-^{32}P]ATP. After PNK had been heat inactivated, free ATP was removed on a Microspin G-25 column. Nicked substrates (Figure 1) were

assembled at room temperature by combining upstream 26mer with 45mer template and 5′-phosphorylated downstream 19mer at a ratio of 1:1.2:1.44; heating and slow cooling the substrate to effect complete annealing were found to be unnecessary. Substrates were predominantly constructed with the ^{32}P label at the 5′ terminus of the upstream 26mer. However, this occasionally allowed blunt end ligation to occur (for those base pairs displaying a very high K_M and therefore requiring high nicked DNA concentrations to saturate the enzyme). When this was the case, the ^{32}P label was placed at the 5′ terminus of the downstream 19mer using PNK to catalyze the exchange reaction. On average, only 2% of the substrate molecules were labeled. Prior to storage at 4 °C, substrate was diluted to a concentration of 5−30 μM using the following buffer: 50 mM Tris-borate, 100 mM KCl, and 15% glycerol (pH → 7.8 with KOH while at 37 °C).

Herein, the base pair identity at the 3′-OH side of a nick is described as X:Y, where X represents the templating nucleotide and Y is the nucleotide that would have been inserted by a polymerase in the preceding gap-filling step. Note that this notation is the reverse of what has occasionally been used in the DNA ligase literature, but is consistent with the notation commonly used in studies of DNA polymerases. The sequences of the oligonucleotides used to assemble all 16 different substrates (four Watson−Crick pairs and 12 mismatches) are listed in Figure 1. To facilitate comparison of mismatch formation and utilization by Pol X and ASFV DNA ligase, the 45mer templates used here are identical to those used in our previous kinetic analysis of Pol X (*9*). The presence of two slightly different classes of ligation substrates in Figure 1 is rooted in DNA polymerase methodology. When polymerase-catalyzed single-nucleotide incorporation is monitored on a template−primer substrate, the nascent templating nucleotide must be different than the templating nucleotide 5′ to it to prevent multiple incorporation events. It is for this reason, along with our intention to make comparisons between Pol X and ASFV DNA ligase, that two slightly different templating sequences were employed in these studies.

Assay Buffer Optimization. "Base buffer" consisted of 50 mM Tris-borate, 50 mM KCl, and 3% glycerol (pH → 7.8 with KOH while at 37 °C), supplemented with 1 mM ATP, 10 mM $MgCl_2$, 100 μM DTT, and 100 μg/mL BSA. Ligation of the nicked G:C substrate, present at a concentration of 100 nM, was monitored at 37 °C in the titrations described below. The one exception was that in the KCl titration the nicked C:G base pair was used instead of the nicked G:C base pair. Magnesium titration: base buffer but with $MgCl_2$ at a total concentration of 5, 7.5, 10, 13.3, 16.6, or 20 mM. BSA titration: base buffer but with BSA at a concentration of 0, 0.05, 0.1, 0.2, 0.4, 0.8, 1.6, 4, 8, 16, 32, or 62.5 mg/mL. KCl titration: base buffer but with KCl at 25, 45, 65, 85, 105, 125, 145, 175, 215, 265, or 325 mM. Glycerol titration: base buffer but with glycerol at 0, 0.5, 1, 2, 4, 8, 16, or 32% (v/v), and 2 mg/mL BSA and 15 mM $MgCl_2$. DTT titration: base buffer but with DTT at a concentration of 0, 0.05, 0.1, 0.3, 0.6, 2, 10, or 20 mM, and 2 mg/mL BSA and 15 mM $MgCl_2$.

Enzyme Assays. Unless noted otherwise, all DNA ligase assays for determining active enzyme concentrations and for fidelity analyses were performed at 37 °C in the optimized buffer consisting of 50 mM Tris-borate, 100 mM KCl, and 15% glycerol (pH → 7.8 with KOH while at 37 °C) with 15 mM $MgCl_2$, 1 mM ATP, 300 μM DTT, and 1.5 mg/mL BSA. All reactions were conducted manually. After a 5 min preincubation at 37 °C, a solution containing DNA ligase, $MgCl_2$, ATP, DTT, and BSA at twice the intended concentrations was added to an equal volume of nicked DNA substrate, also at twice the intended concentration. Generally, 10 μL aliquots were removed at the appropriate time points and quenched in 10 μL of formamide containing xylene cyanol and bromophenol blue. Reaction products were resolved on 15% denaturing polyacrylamide gels and visualized by phosphor screen autoradiography using a STORM840 scanner from Molecular Dynamics. Band intensity quantitation and data plotting were carried out with ImageQuant and SigmaPlot, respectively.

Saturation curves were obtained by plotting the initial velocity (v_0) as a function of substrate concentration and fitting the data to the Michaelis−Menten equation: $v_0 = V_{max}[S]/(K_m + [S])$. k_{cat} was obtained by dividing V_{max} by the enzyme concentration. Each saturation curve was repeated at least twice, and the reported data represent the single best independent trial. Each saturation curve contained v_0 values for seven different substrate concentrations, as shown in the Results. For most of the 32 saturation curves that were generated (16 for each enzyme), the highest substrate concentration used was greater than $5K_M$. Enzyme concentrations were varied (between 52 pM and 19 nM for T4 ligase and between 64 pM and 31 nM for ASFV DNA ligase) for each substrate so that time points, corresponding to less than 30% turnover, could be taken in the range of 10 s to 1 h.

Determining the Concentration of Active T4 DNA Ligase. Since the T4 DNA ligase stock used in our studies contained BSA (added by the vendor to help stabilize the enzyme), UV absorbance was never used for the initial approximation of enzyme concentration. The T4 DNA ligase burst assay employed a 200-fold dilution of the enzyme stock (concentration unknown at this point; this assay's purpose was to quantitate the active enzyme concentration) and a nicked substrate (at 1180 nM) containing a 5′-phosphate and a 3′-amino group (in place of a 3′-hydroxyl). Data from this assay were fit to the burst equation as indicated in the Results. The 3′-amino-terminated oligonucleotide was synthesized by Pol β-catalyzed incorporation of 2′-deoxy-3′-aminocytidine triphosophate into the appropriate gapped substrate. This 3′-amino-terminated 26mer was gel purified, quantitated, and then assembled into a nicked substrate as outlined above; it was similar to the G:C substrate shown in Figure 1 except that the 5′ ^{32}P label was placed on the downstream 19mer using PNK to catalyze the exchange reaction.

Determining the Concentration of Active ASFV DNA Ligase. As do most, if not all, purified DNA ligases, ASFV DNA ligase exists in two distinct forms: one without the AMP (adenylyl) cofactor and one with the adenylyl group covalently bound to a catalytic lysine (in Figure 2 these are represented by the first and second species, respectively). We say that the total concentration of the active (natively folded) enzyme is equal to the sum of the active adenylylated and active unadenylylated forms:

$$[E]_{active,total} = [E]_{active,adenylylated} + [E]_{active,unadenylylated} \quad (1)$$

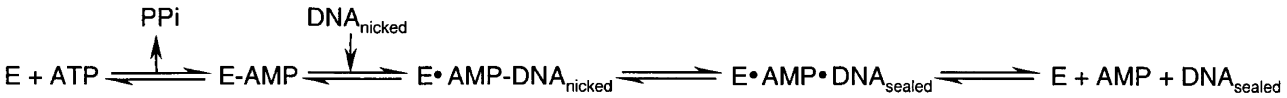

FIGURE 2: Simplified ATP-dependent DNA ligase mechanism. A catalytic lysine attacks the α-phosphate of ATP, generating a lysyl-AMP adduct and releasing pyrophosphate. The conformational change that is apparently induced during this step is not indicated in this scheme. Adenylylated ligase then binds nicked DNA and transfers the AMP group from lysine to the 5′-phosphate of the nick. The 3′-hydroxyl of the nick then attacks the adenylylated 5′-phosphate, forming a phosphodiester bond and eliminating AMP. Finally, the cofactor and sealed DNA product are released.

To determine the concentration of "charged" (adenylylated) ASFV DNA ligase, the enzyme (at roughly 20 nM) was incubated with 100 nM nicked G:C substrate in assay buffer lacking ATP. These data were fit to the single-exponential equation [product] = $A[1 - \exp(-k_{obs}t)]$, where A represents the single-turnover amplitude and k_{obs} is the observed rate constant. $[E]_{active,adenylylated}$ was determined by multiplying the single-turnover amplitude by the enzyme dilution factor.

$[E]_{active,unadenylylated}$ was determined indirectly using synthetic, nicked DNA in which the 5′-phosphate was linked to the phosphate moiety of AMP. This substrate represents the DNA ligase reaction intermediate formed immediately prior to nick sealing (Figure 2) and will be termed adenylylated DNA or adenylylated substrate. With the exception of the extrahelical 5′-adenylyl group, this substrate was similar to the G:C substrate shown in Figure 1. Parallel reactions with adenylylated DNA were performed in assay buffer lacking ATP and had the following format. ASFV DNA ligase was preincubated for 15 min in the absence (assay 1) or presence (assay 2) of 450 nM unlabeled, nicked DNA and then mixed with the ^{32}P-labeled, adenylylated substrate. The final concentrations of enzyme and adenylylated DNA were 240 pM and 590 nM, respectively. In assay 1, both the adenylylated and unadenylylated forms of the ligase persist after the preincubation step. Upon addition of the adenylylated substrate, only the unadenylylated form of the enzyme shows turnover (the 5′-adenylyl moiety on the DNA precludes binding by adenylylated ligase). From this assay, we obtained an initial velocity, $v_{0,unadenylylated}$. In assay 2, the nicked DNA present during the preincubation effects deadenylylation of the ligase. Accordingly, upon addition of the adenylylated substrate, all active ligase molecules show turnover, allowing determination of the initial velocity $v_{0,total}$. The $v_{0,total}/v_{0,unadenylylated}$ ratio is equivalent to the $[E]_{active,total}/[E]_{active,unadenylylated}$ ratio, allowing us to write the expression $[E]_{active,total} = n[E]_{active,unadenylylated}$, where n is the empirically determined proportionality constant. This expression can be substituted into eq 1, along with the value of $[E]_{active,adenylylated}$ (from the single-turnover experiment), to determine the concentration of the unadenylylated form of the protein.

For the preincubation step described above, 450 nM unlabeled, nicked DNA was empirically determined to be the optimal concentration, giving the greatest extent of "activation" relative to the sample not exposed to nicked DNA during preincubation, by varying the concentration of unlabeled, nicked DNA. The different concentrations examined were 0.6, 1.2, 12, 70, 120, 200, 300, 450, and 1200 nM.

RESULTS

Assay Buffer Optimization. ASFV DNA ligase was initially assayed in buffer similar to that which had been used in studies of Pol X (*9*): 50 mM Tris-borate, 50 mM KCl, and 3% glycerol (pH → 9.0 with KOH at room temperature) supplemented with 10 mM $MgCl_2$, 1 mM ATP, 100 μM DTT, and 100 μg/mL BSA. However, under these conditions, the activity of ASFV DNA ligase was low and data were difficult to reproduce. Subsequently, a cursory pH titration demonstrated the enzyme to have optimal activity in the pH range of 7.5−8.5, with activity decreasing dramatically above pH 8.75 (data not shown). Accordingly, the pH was fixed at 7.8, and individual buffer components were titrated (parts A−E of Figure 3) as described in Experimental Procedures. On the basis of these titrations, the following optimal buffer was chosen: 50 mM Tris-borate, 100 mM KCl, and 15% glycerol (pH → 7.8 with KOH while at 37 °C) with 15 mM $MgCl_2$, 1 mM ATP, 300 μM DTT, and 1.5 mg/mL BSA. In addition to approximating the physiological pH and potassium concentration, these conditions also afforded increased activity for ASFV DNA ligase and excellent reproducibility of kinetic data. T4 DNA ligase exhibited good activity in the optimized ASFV DNA ligase assay buffer, allowing the two enzymes to be studied under identical conditions.

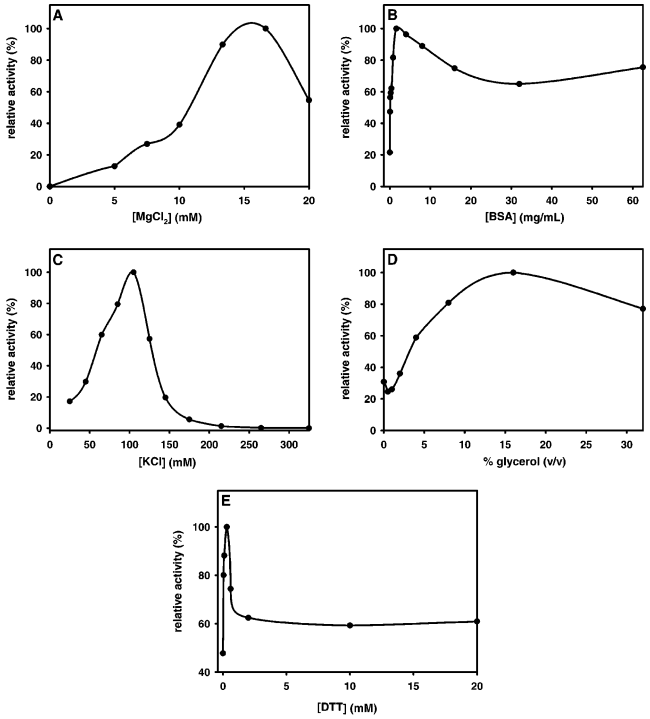

FIGURE 3: Optimization of DNA ligation assay buffer. ASFV DNA ligase was assayed for its ability to seal 100 nM nicked substrate as a function of $MgCl_2$ concentration (A), BSA concentration (B), KCl concentration (C), percent glycerol (D), and DTT concentration (E). Details for each of these titrations are listed in Experimental Procedures.

Determining the Concentration of Active DNA Ligase. It is often the case for recombinant enzymes that the UV-determined protein concentration is considerably higher than

that determined by kinetic analyses, indicating that not all of the purified protein is active and/or that contaminant protein is present. This technical difficulty is compounded for DNA ligases since the active, natively folded form of these enzymes exists as a mixture of a catalytically competent form (with the AMP cofactor covalently bound) and a catalytically incompetent form (lacking the cofactor) (Figure 2). Most previous studies of DNA ligases have not required an accurate knowledge of the concentration of active enzyme (in either of its forms) and have simply used UV-approximated values. To ensure that the k_{cat} values reported here were as accurate as possible, we developed novel assays (described below) for determining active enzyme concentrations; to our knowledge, these represent the most rigorous, and also the most practical, methods available for determining the concentration of a DNA ligase.

As the first step of a DNA ligation reaction, the ϵ-NH_2 group of a lysine residue attacks the α-phosphate of ATP (or the pyrophosphate linkage of NAD^+), forming an enzyme−AMP intermediate (Figure 2) (*14*). This "charging" process appears to effect structural rearrangements which facilitate binding of nicked DNA (*15*). The AMP moiety is subsequently transferred to the 5′-phosphate of a DNA nick, thereby activating the 5′-phosphate for nucleophilic attack by the adjacent 3′-hydroxyl (*14*). DNA ligases are expected to exist in vivo as a mixture of both the adenylylated ("charged") and unadenylylated ("uncharged") forms. Upon overexpression and subsequent purification, the ratio of these forms can vary dramatically depending on the identity of the particular enzyme, the expression host, the method of purification, etc.

One approach for determining the total concentration of active DNA ligase would be to quantitatively precharge the enzyme and then incubate it with nicked DNA under conditions that either result in a single turnover or that force the enzyme to show burst kinetic behavior. As shown in parts A and B of Figure 4, when incubated with nicked DNA containing a 3′-NH_2 group in place of the canonical 3′-OH, T4 DNA ligase adenylylates the 5′-phosphate of the nick in a rapid single turnover that is followed by a slower steady-state phase. These data were fit to the burst equation $[\text{product}] = A[1 - \exp(-k_{obs}t)] + ct$, where A is the burst amplitude, k_{obs} is the observed single-exponential rate constant, and c is the steady-state rate of transferring AMP from the AMP ligase to nicked DNA. The steady-state rate constant (k_{ss}) was obtained by dividing c by A. For the plot in Figure 4B, $A = 60.6$ nM, $k_{obs} = 1.63$ min^{-1}, and $k_{ss} = 0.016$ min^{-1}. Since the enzyme was preincubated with ATP prior to mixing with DNA (allowing all active protein molecules to become charged), and since 1180 nM 3′-amino-terminated substrate was found to be sufficient for saturating T4 ligase, the burst amplitude corresponds to the total concentration of the active enzyme in this assay. Multiplying the burst amplitude by the enzyme dilution factor for this assay (200-fold dilution) indicated that for this particular stock of T4 DNA ligase $[E]_{active,total} = 12.12$ μM.

In contrast to T4 DNA ligase, ASFV DNA ligase adenylylated the 3′-amino-containing substrate extremely inefficiently, with reactions typically proceeding to only ~5% completion, and did not show burst behavior. It is worth noting that burst behavior was not observed, and the efficiency of DNA adenylylation was dramatically reduced,

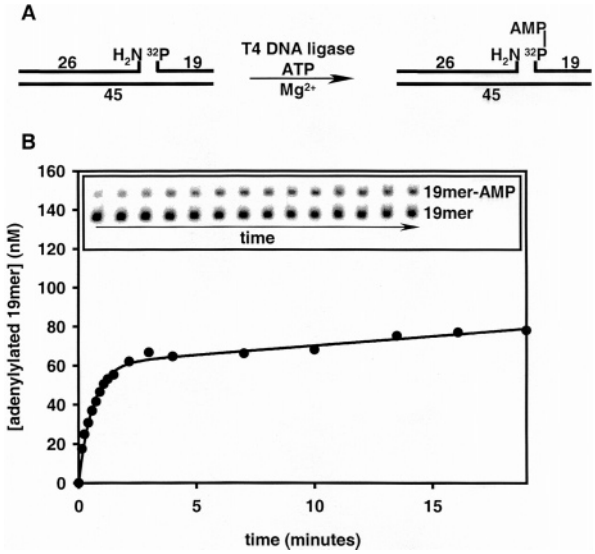

FIGURE 4: Burst assay to determine the total concentration of active T4 DNA ligase. (A) When using a 3′-amino-containing nick, T4 DNA ligase catalyzes transfer of the adenylyl group from the enzyme's catalytic lysine to the 5′-phosphate of the nick. Using this unnatural substrate, the final nick-sealing step is blocked, allowing the adenylylated DNA intermediate to accumulate. (B) Biphasic behavior of T4 DNA ligase acting on a 3′-amino-containing nick (present at 1180 nM). Data (●) were fit to the burst equation; kinetic parameters, included the empirically determined enzyme concentration, are listed in the Results. The gel displayed in the inset shows accumulation of the adenylylated DNA intermediate as a function of time.

when T4 or ASFV DNA ligases were incubated with a 3′-H (dideoxy)-containing nick (data not shown). Similar results have been obtained for other DNA ligases (*16*), including the NAD^+-dependent enzyme from *Escherichia coli* (*17*). Collectively, these data may suggest that the 3′-OH of the nick coordinates a catalytic magnesium ion during transfer of the adenylyl group from lysine to the 5′-phosphate of the nick; in its unprotonated state, the 3′-amino group possesses a lone pair of electrons capable of coordinating a magnesium ion, whereas such coordination by the 3′-hydrogen in the dideoxy-terminated nick is not possible. It is worthwhile to note that Lee and co-workers previously postulated that the 3′-OH of a nick may coordinate a catalytic magnesium ion during the third (nick sealing) step of DNA ligation (*18*); a recent crystal structure of human DNA ligase I complexed with adenylylated DNA is consistent with this (*19*). As an alternative to magnesium coordination, the 3′ moiety of the nick might serve as a hydrogen bond donor and/or acceptor, helping to position active site residues during the DNA adenylylation step.

Since ASFV DNA ligase did not exhibit biphasic kinetics with the amino-terminated substrate, an alternative set of three assays was employed for determining the total concentration of the active enzyme. The concentration of the active, adenylylated enzyme was determined by the amplitude of a single-turnover assay in which the enzyme was incubated with nicked DNA in the absence of exogenous ATP (Figure 5A). Data points were fit to the single-exponential equation $[\text{product}] = A[1 - \exp(-k_{obs}t)]$, where A is the single-turnover amplitude (14.4 nM) and k_{obs} is the observed rate constant (1.99 min^{-1}). Since the enzyme was diluted 75-fold in this particular assay, $[E]_{active,adenylylated} = 1.08$ μM.

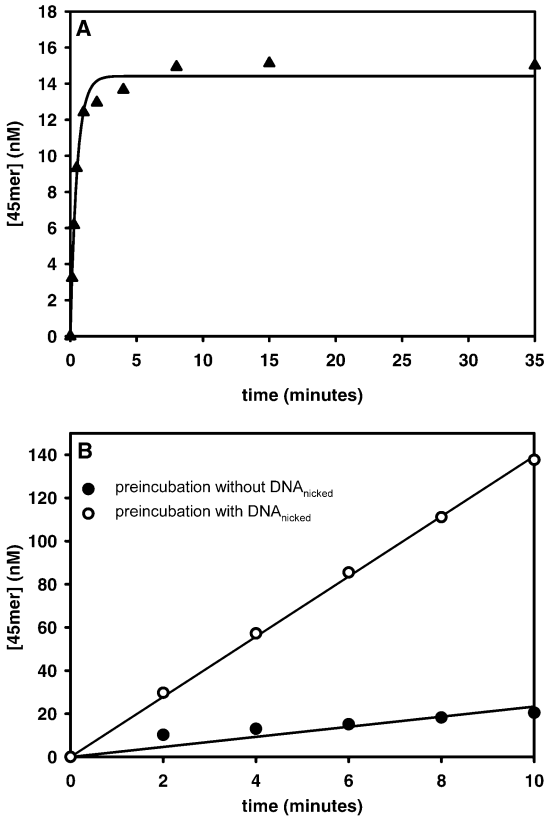

FIGURE 5: Three assays to determine the concentration of active ASFV DNA ligase in both the adenylylated and unadenylylated forms. (A) Determination of the concentration of adenylylated ASFV DNA ligase. A single turnover was performed by incubating ASFV DNA ligase with 100 nM nicked G:C substrate in the absence of ATP. The data (▲) were fit to a single exponential; kinetic parameters, including the empirically determined enzyme concentration, are listed in the Results. (B) Determination of the concentration of unadenylylated ASFV DNA ligase. Steady-state ligation of 590 nM adenylylated DNA by 240 pM ASFV DNA ligase after a preincubation with (○; $v_{0,total}$ = 13.94 nM/min) or without (●; $v_{0,unadenylylated}$ = 2.33 nM/min) 450 nM unlabeled, nicked DNA. As outlined in Experimental Procedures and demonstrated in the Results, these initial velocities were used, along with the single-turnover amplitude from part A, to determine the concentration of active, unadenylylated enzyme.

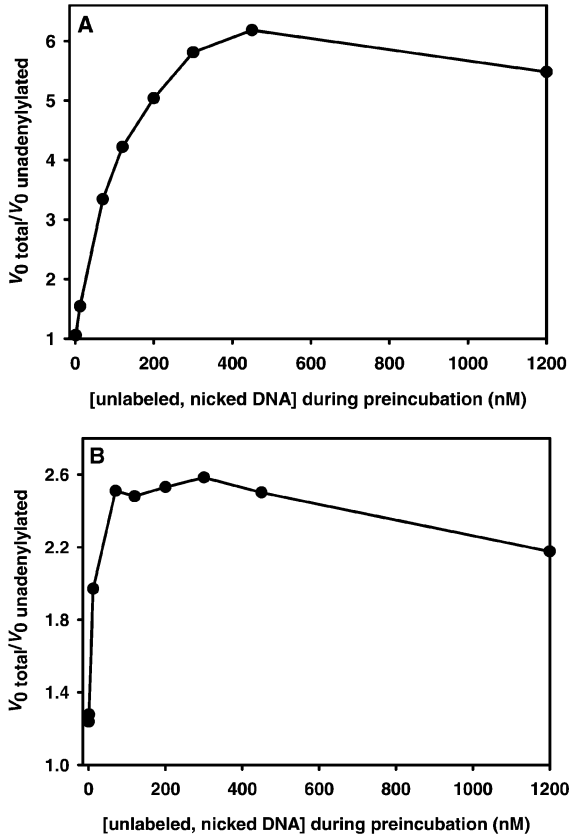

FIGURE 6: Empirical determination of the optimal nicked substrate concentration for deadenylylating DNA ligase prior to incubation with the adenylylated substrate. As in the assay shown in Figure 5B, the initial velocity (v_0) of ligating adenylylated DNA was monitored after the enzyme was preincubated with unlabeled, nicked DNA (giving $v_{0,total}$) or after the enzyme was preincubated without unlabeled, nicked DNA (giving $v_{0,unadenylylated}$). See Experimental Procedures for details. The ratio $v_{0,total}/v_{0,unadenylylated}$ is plotted as a function of the concentration of unlabeled, nicked substrate used during the preincubation step for ASFV DNA ligase (A) and T4 DNA ligase (B).

An adenylylated DNA substrate (see Experimental Procedures) was then employed in two separate assays to determine, indirectly, the concentration of active, unadenylylated enzyme. When incubated with this adenylylated substrate in the absence of ATP, only the unadenylylated ligase molecules show turnover, giving an initial velocity $v_{0,unadenylylated}$ of 2.33 nM/min (Figure 5B). However, after a preincubation with 450 nM unlabeled, nicked DNA, to decharge the adenylylated form of the ligase, all of the enzyme molecules are able to turn over the adenylylated substrate, giving an initial velocity $v_{0,total}$ of 13.94 nM/min (Figure 5B). As outlined in Experimental Procedures, the difference in the initial velocity of these two reactions can be used to determine the concentration of each form of the enzyme. We have $v_{0,total}/v_{0,unadenylylated} = 5.98 = [E]_{active,total}/[E]_{active,unadenylylated}$. Substitution into eq 1, along with the $[E]_{active,adenylylated}$ value determined above, gives an $[E]_{active,unadenylylated}$ of 217 nM. Accordingly, 83% of the enzyme existed in the adenylylated form after expression in *E. coli* and subsequent purification.

The concentration of unlabeled, nicked DNA used in the preincubation step described above was not arbitrarily chosen to be 450 nM. If present at an overly low concentration, this substrate would not effect complete deadenylylation of the ligase. If present at an overly high concentration, the residual nicked molecules from the preincubation step might subsequently inhibit ligation of the labeled, adenylylated substrate. To determine what substrate concentration in the preincubation step would optimally "activate" ASFV DNA ligase, the ratio $v_{0,total}/v_{0,unadenylylated}$ was monitored for a series of reactions in which the concentration of unlabeled, nicked substrate in the preincubation step was varied between 0.6 and 1200 nM. Figure 6A suggests that when the substrate concentration during the 15 min preincubation is below 450 nM, ASFV DNA ligase is not quantitatively deadenylylated. The decrease in $v_{0,total}/v_{0,unadenylylated}$ on going from 450 to 1200 nM substrate is consistent with ligation of the labeled, adenylylated substrate being inhibited by the unlabeled, nicked substrate molecules left over from the preincubation. Accordingly, it appears that unadenylylated ASFV DNA ligase does interact with nicks, albeit with a reduced affinity.

The optimal concentration of unlabeled, nicked DNA to be used in the preincubation step is expected to vary from one DNA ligase to the next, being a function of the enzyme's

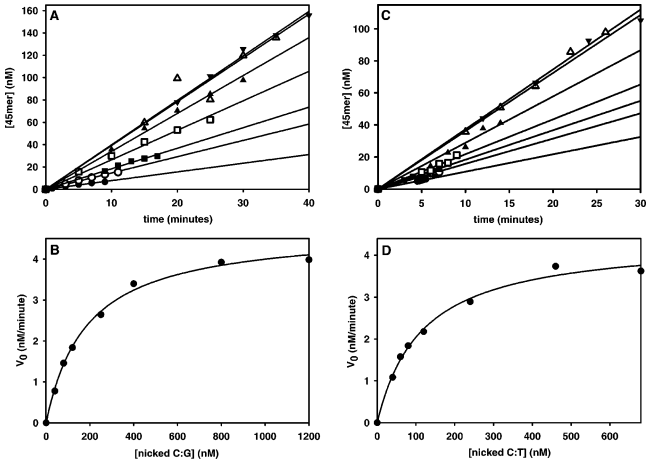

FIGURE 7: Two saturation curves for ASFV DNA ligase. (A) Sealing the nicked C:G substrate as a function of time. Substrate concentrations were 40 (●), 80 (○), 120 (■), 250 (□), 400 (▲), 800 (△), and 1200 nM (▼). Lines are linear fits forced through the origin. (B) Initial velocities from part A plotted as a function of substrate concentration. Data points (●) were fit to the Michaelis−Menten equation as outlined in Experimental Procedures. Kinetic parameters are listed in Table 2. (C) Sealing the nicked C:T mismatch as a function of time. Substrate concentrations were 40 (●), 60 (○), 80 (■), 120 (□), 240 (▲), 460 (△), and 680 nM (▼). Lines are linear fits forced through the origin. (D) Initial velocities from part C plotted as a function of substrate concentration. Data points (●) were fit to the Michaelis−Menten equation as described above.

affinity for the different DNA species. To test this, an identical set of assays were performed with T4 DNA ligase (Figure 6B). Though the curves in parts A and B of Figure 6 have similar shapes, the T4 enzyme is optimally activated by 300 nM substrate during the preincubation (vs 450 nM for the ASFV enzyme). Importantly, summation of the $[E]_{active,unadenylylated}$ determined for T4 ligase (using 300 nM substrate during the preincubation) with the $[E]_{active,adenylylated}$ obtained from a single turnover (data not shown) gave an $[E]_{active,total}$ of 11.91 μM, which differs from the value determined by the burst assay (12.12 μM) by less than 2%. Such a high level of convergence from two independent methodologies suggests that both provide an accurate measure of the active DNA ligase concentration.

DNA Nick Ligation Assays. ASFV DNA ligase was assayed in the steady state to generate saturation curves (see Figure 7 for two examples) for nicked substrates containing all 16 possible base pair combinations at the 3′-OH side of the nick (substrate details are shown in Figure 1). Having previously been described as a low-fidelity DNA ligase (*12*), on the basis of its limited discrimination against a 3′ G:T mismatch, T4 DNA ligase was also assayed to serve as a reference. For both of these enzymes, catalytic efficiency is plotted as a function of base pair in parts A and B of Figure 8. When compared with T4 DNA ligase (Table 1), ASFV DNA ligase (Table 2) displays a lower fidelity, defined as $(k_{cat}/K_M)_{correct}/(k_{cat}/K_M)_{incorrect}$, for sealing 11 of the 12 possible mismatched nicks. Especially salient is the fact that the ASFV enzyme ligates the C:T mismatch 3-fold more efficiently than the corresponding Watson−Crick base pair, C:G (Figure 8B and Table 2). This preference for the C:T mismatch results from both a higher k_{cat} and a lower K_M, relative to those of the C:G base pair. This is the first reported example of a DNA ligase that preferentially seals a mismatched nick. Comparison with previous examinations of DNA ligase fidelity (*12*, *20*) indicates that ASFV DNA ligase

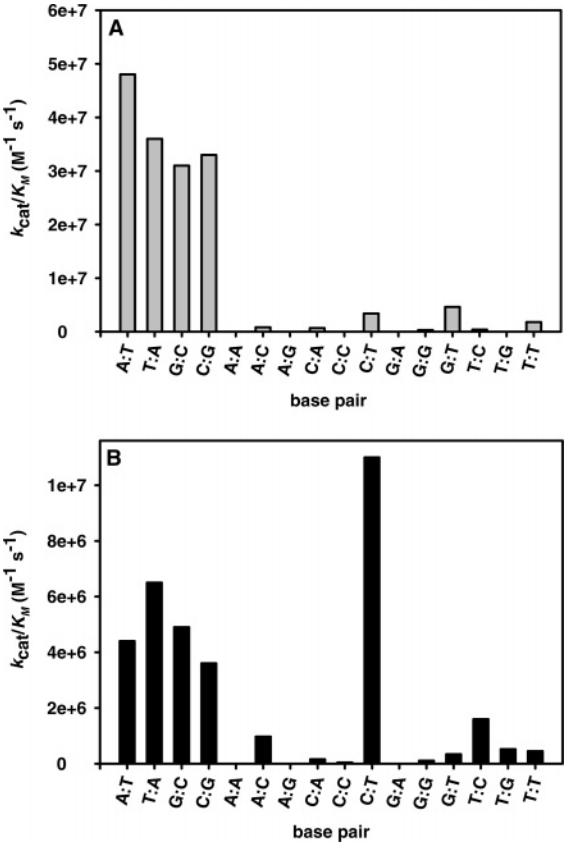

FIGURE 8: Catalytic efficiency of nick sealing, as a function of base pair, for T4 and ASFV DNA ligases. Each of the 16 possible base pair combinations at the 3′-OH side of a nick was examined (see Figure 1 for substrate details). Base pairs are described using the notation X:Y, where X designates the templating position and Y denotes the nucleotide that would have been inserted by a polymerase in the preceding gap-filling step: (A) T4 DNA ligase and (B) ASFV DNA ligase. Note the different scales for the *y*-axes.

Table 1: Kinetic Parameters for Nick Ligation by T4 DNA Ligase as a Function of 3′ Base Pair Identity

base pair[a]	k_{cat} (s^{-1})	K_M (nM)	k_{cat}/K_M (M^{-1} s^{-1})	fidelity[b]
A:T	3.5 ± 0.29	74 ± 15	4.7×10^7	−
A:C	0.23 ± 0.011	280 ± 47	8.2×10^5	57
A:A	0.043 ± 0.0011	680 ± 62	6.3×10^4	750
A:G[c]	0.049 ± 0.053	290000 ± 320000	1.7×10^2	280000
T:A	6.0 ± 0.22	170 ± 24	3.5×10^7	−
T:T	0.26 ± 0.0066	150 ± 12	1.7×10^6	21
T:C	0.51 ± 0.030	1300 ± 240	3.9×10^5	90
T:G	0.22 ± 0.0090	1100 ± 140	2.0×10^5	180
G:C	4.9 ± 0.23	160 ± 22	3.1×10^7	−
G:T	2.9 ± 0.11	640 ± 62	4.5×10^6	6.9
G:G	0.46 ± 0.018	1600 ± 140	2.9×10^5	110
G:A	0.015 ± 0.0014	2600 ± 570	5.8×10^3	5300
C:G	7.2 ± 0.10	220 ± 8.7	3.3×10^7	−
C:T	3.2 ± 0.075	940 ± 59	3.4×10^6	9.7
C:A	0.51 ± 0.035	750 ± 140	6.8×10^5	49
C:C	0.048 ± 0.0056	3500 ± 860	1.4×10^4	2400

[a] In the base pair notation X:Y, X refers to the templating nucleotide and Y is the nucleotide that would have been inserted by a polymerase in the preceding gap-filling step (see Figure 1 for structures). [b] Fidelity is defined as $(k_{cat}/K_M)_{correct}/(k_{cat}/K_M)_{incorrect}$. [c] T4 DNA ligase seals the A:G mismatch extremely inefficiently. At 10 μM A:G substrate, the enzyme was nowhere close to being saturated. Thus, the k_{cat} and K_M values reported for this substrate were obtained by considerable extrapolation.

Table 2: Kinetic Parameters for Nick Ligation by ASFV DNA Ligase as a Function of 3′ Base Pair Identity

base pair[a]	k_{cat} (s^{-1})	K_M (nM)	k_{cat}/K_M (M^{-1} s^{-1})	fidelity[b]
A:T	0.80 ± 0.089	180 ± 50	4.4×10^6	–
A:C	0.28 ± 0.0090	290 ± 33	9.7×10^5	4.5
A:A	0.041 ± 0.00065	2100 ± 77	2.0×10^4	220
A:G	0.00093 ± 0.000050	1600 ± 270	5.8×10^2	7600
T:A	0.81 ± 0.058	130 ± 27	6.2×10^6	–
T:T	0.27 ± 0.023	580 ± 160	4.7×10^5	13
T:C	0.37 ± 0.025	240 ± 53	1.5×10^6	4.1
T:G	0.27 ± 0.014	510 ± 110	5.3×10^5	12
G:C	1.0 ± 0.04	200 ± 30	5.0×10^6	–
G:T	0.35 ± 0.028	1000 ± 200	3.5×10^5	14
G:G	0.24 ± 0.0047	2100 ± 83	1.1×10^5	45
G:A	0.014 ± 0.00068	1100 ± 210	1.3×10^4	380
C:G	0.67 ± 0.017	180 ± 14	3.7×10^6	–
C:T	1.2 ± 0.043	120 ± 11	1.0×10^7	0.37
C:A	0.16 ± 0.011	1000 ± 230	1.6×10^5	23
C:C	0.059 ± 0.0015	1400 ± 99	4.2×10^4	88

[a] In the base pair notation X:Y, X refers to the templating nucleotide, and Y is the nucleotide that would have been inserted by a polymerase in the preceding gap-filling step (see Figure 1 for structures). [b] Fidelity is defined as $(k_{cat}/K_M)_{correct}/(k_{cat}/K_M)_{incorrect}$.

has, by far, the lowest fidelity of any DNA ligase reported to date.

To assess the precision of the fidelity values reported here, the activity of ASFV DNA ligase against the nicked C:G and C:T base pairs was reexamined using substrates assembled from different preparations of the component oligonucleotides (identical sequences, but the oligonucleotide stocks were different than those used in generating data for Table 2). From this set of assays, the fidelity of nicked C:T ligation by ASFV DNA ligase was determined to be 0.41. This compares very well with the value of 0.37 in Table 2, confirming the C:T base pair preference of ASFV DNA ligase and suggesting a precision of roughly ±10% for the reported fidelity values.

A few noteworthy trends emerging from the data in Figure 8 and Tables 1 and 2 are as follows. First, T4 DNA ligase seals correctly matched nicks between 6- and 11-fold more efficiently than ASFV DNA ligase; this difference is largely attributable to the higher k_{cat} values of the T4 enzyme (Tables 1 and 2). Second, base pair size or geometry appears to be an important determinant of ligation efficiency. Consistent with what has been published for a diverse set of DNA ligases (*21*−*24*), ASFV and T4 DNA ligases seal the bulky 3′ purine:purine mismatches (A:A, G:G, G:A, and A:G) very inefficiently. In contrast, the purine:pyrimidine, pyrimidine:purine, and pyrimidine:pyrimidine mismatches tend to be better tolerated. Though the literature shows that the preferred 3′ mismatch varies from one enzyme to the next, G:T, T:G, C:T, and T:C base pairs have generally proven to be well tolerated (*21*−*23*), and this is also the case for the two enzymes described here. Note, however, that the efficiency of sealing the two permutations of a given base pair, such as the mismatched C:T and T:C, can vary considerably, indicating that simple base pair shape or geometry is not the sole determinant of ligation efficiency.

On the basis of our kinetic data, it is clear that discrimination against mismatches occurs both at the level of nick binding and during the chemical steps (one or both of the adenylyl transfers involving the DNA nick). This is particularly evident among the four purine:purine mismatches and the C:C mismatch, all of which display extremely high K_M values and low k_{cat} values with both T4 and ASFV DNA ligases.

Mismatch discrimination at the level of DNA binding has recently been examined using nucleotide analogues with Tth DNA ligase. Liu and co-workers demonstrated that, as in many DNA polymerases, the relative positioning of minor groove hydrogen bond acceptors (N3 of the purines and the C2 carbonyl of the pyrimidines) is a critical factor in deciphering between match versus mismatch at the 3′ base pair of a nick (*25*). It will be interesting to see whether this is a universal fidelity determinant among DNA ligases and, if so, how the ASFV enzyme has redirected its specificity to accommodate 3′ mismatches while still sealing the canonical Watson−Crick base pairs.

Inversion of stereochemistry during the third step (nick sealing) of DNA ligation by T4 ligase (*26*) is consistent with an associative in-line attack of the 5′-phosphate by the 3′-hydroxyl; it is assumed that all ligases operate by a similar mechanism. The relative positions of the 5′-phosphate and the 3′-hydroxyl are expected to fluctuate with the identity of the 3′ base pair. Since ASFV DNA ligase displays an enhanced k_{cat} with the pyrimidine:pyrimidine C:T mismatch (relative to that of C:G), it would appear that this enzyme repositions these reactive groups on the annealed, nicked substrate to facilitate chemistry. The mechanism by which this is accomplished is of particular interest.

Nick Ligation Fidelity as a Function of Ionic Strength. Lindahl and co-workers demonstrated that the concentration of KCl used in their assay buffer dramatically influenced the fidelity of DNA ligation for human DNA ligases I and III (*20*). We have found this to also be true for ASFV DNA ligase; the fidelity for sealing the C:T mismatch is higher at 150 mM KCl than it is at 100 mM KCl. However, even at 150 mM KCl, the C:T mismatch is still sealed more efficiently than the correctly matched C:G. Though a number of examples of 3′ mismatch tolerance by a DNA ligase have been described in the literature, these studies have been conducted at low, nonphysiological ionic strengths (*21*−*23*, *27*, *28*). Despite the fact that these artificial conditions often enhance mismatch ligation efficiency, in no case did the ligase being studied actually seal a mismatch preferentially, highlighting the uniqueness of the ASFV enzyme described in this report.

DISCUSSION

Determining Active DNA Ligase Concentrations. When T4 DNA ligase is incubated with a 3′ amino-terminated nick, the second step of nick sealing (DNA adenylylation; see Figure 2) proceeds with high efficiency while the third step (nick sealing) is blocked altogether. This gives rise to biphasic kinetic behavior where the steady-state phase is limited by dissociation of the enzyme·AMP-DNA complex or a conformational change associated with this. Since the enzyme is preincubated with ATP, thereby quantitatively charging it, before being mixed with DNA, the amplitude of the burst gives the total concentration of the active enzyme. As suggested by the differences observed between ASFV and T4 DNA ligases, 3′-amino-containing nicked substrates may give rise to burst kinetic behavior among only a subset of DNA ligases.

While it is well-known that DNA ligases can bind to and seal adenylylated DNA (*17*, *29*), herein we took advantage

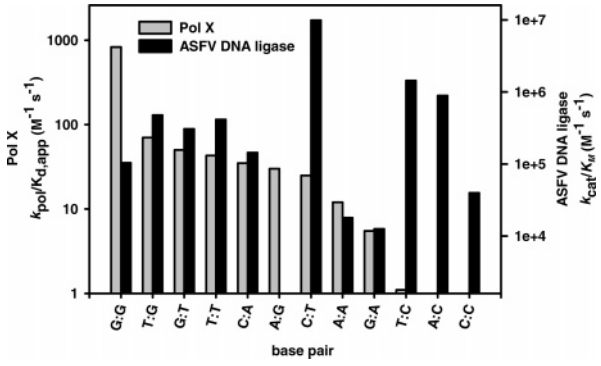

FIGURE 9: Comparison of catalytic efficiencies (mismatches only) for Pol X and ASFV DNA ligase. Base pairs are arranged, from left to right, in order of decreasing Pol X catalytic efficiency for mismatch synthesis (gray bars). The corresponding catalytic efficiency for mismatch ligation by ASFV DNA ligase is also shown (black bars). The two *y*-axes, though different in their magnitudes, are both displayed using a logarithmic scale. Data for Pol X are from ref *9*.

of this property for the purpose of determining the concentration of active enzyme existing in both the adenylylated and unadenylylated states. Because the adenylylated DNA substrate is a universal intermediate in the DNA ligation reaction mechanism, the technique described here using both ASFV and T4 DNA ligases is expected to be broadly applicable for determining the concentration of DNA ligases.

Mismatch Specificity of Pol X versus ASFV DNA Ligase. Nature's selective pressure is ultimately exerted on enzyme systems. Since the genes encoding ASFV Pol X and DNA ligase have presumably coevolved, comparing the mismatch specificities of these two enzymes may provide clues about the selective pressure that has promoted low fidelity in ASFV DNA ligase. If ASFV DNA ligase has evolved toward low fidelity for the purpose of sealing the replisome-blocking lesions (mismatched nicks) generated by Pol X, then its mismatch specificity is expected to be similar to that of Pol X. In this scenario, since persistently unligated mismatched nicks could block genome replication and be lethal to the virus, the ligase should seal most efficiently those mismatches being formed the most frequently by Pol X; as a corollary, mismatches synthesized infrequently by Pol X would be sealed less efficiently by the ligase. While this sort of system would give rise to the largest number of replicatable genomes (i.e., those lacking nicks), it would not generate broad sequence diversity since some sealed mismatches would be overrepresented and others underrepresented. Alternatively, if ASFV DNA ligase has evolved toward low fidelity for the purpose of promoting broad genomic diversity, then the mismatch specificities of these two enzymes are expected to complement one another; those mismatches synthesized least efficiently by Pol X would be sealed very efficiently by ASFV DNA ligase since only in this manner would the entire spectrum of mismatched duplex products be well represented. Note that ASFV does not encode a mismatch repair system or a mismatch-specific glycosylase (*8*) that could repair mismatches after they had been ligated. Figure 9 demonstrates very clearly that the mismatch specificity of ASFV DNA ligase does not mirror the mismatch specificity of Pol X. In contrast, a modest complementation in the mismatch specificities of these two enzymes is observed, with the ligase efficiently sealing the mismatches generated least efficiently by Pol X.

Mutation in ASFV. Though infidelity during replication may in fact contribute to ASFV variability (the ASFV replicative polymerase has not been studied in this regard), we hypothesize that point mutations introduced during DNA repair are likely to contribute to genome diversification in ASFV. That the genes for ASFV Pol X and DNA ligase were initially retained in the ASFV genome suggests the usefulness and/or necessity of these proteins for viral DNA repair (the replacement of a chemically damaged nucleotide with an undamaged nucleotide). That both the Pol X and ASFV DNA ligase proteins are among the most error-prone or error-tolerant members of their respective enzyme families is not likely to be a coincidence and is consistent with these proteins contributing to viral mutagenesis (by replacing a chemically damaged nucleotide with an undamaged, though incorrect, nucleotide).

In contrast to the diversification processes associated with somatic hypermutation (SHM), where error-prone DNA synthesis is targeted to discrete regions of immunoglobulin loci (*30*), the proposed ASFV mutagenic DNA repair system would be capable, in theory, of inducing mutations throughout the entire viral genome. This does not appear to be the case, however, since some regions of the ASFV genome are more prone to variation due to base substitution or small insertions and deletions than are other regions (*1*, *7*). This phenomenon may be a consequence of the mechanism by which the viral genome is replicated and assembled. Short ASFV DNA fragments are present in the host cell nucleus at early stages of virus replication, and subsequently, larger DNA intermediates are detected in the cytoplasm (*5*, *31*). With the ASFV genome being synthesized and assembled via discreet nuclear and cytoplasmic phases of DNA processing, perhaps the extent of DNA damage and the extent of DNA repair by either host nuclear repair factors or ASFV repair factors dictate the location, extent, and type of mutations sustained by the viral genome. This might explain some of the apparent inconsistencies in the literature regarding the variability of ASFV.

A complete DNA repair system remains to be established in ASFV. A DNA glycosylase, capable of removing a chemically modified base to generate an abasic site, has not been identified using homology searches of the ASFV genome (*8*). Accordingly, spontaneously generated abasic sites (*32*) might serve as the initiating lesions in ASFV DNA repair. These could be incised by the putative ASFV APE and the resulting single nucleotide gap filled by Pol X. Prior to nick ligation, however, the 5′-deoxyribose phosphate (5′-dRP) generated by APE incision of the sugar−phosphate backbone would need to be removed. To date, a 5′-dRP lyase or hydrolase has not been identified in ASFV. Though 5′-dRP can be lost spontaneously via β-elimination, the half-life of this reaction under physiological conditions is on the order of 30 h (*33*), representing a severe bottleneck in the APE-initiated route of abasic site repair. Sustained effort will likely result in either the identification of these currently "missing" activities or the elucidation of a permutation of canonical repair pathways. Regardless, the utility to ASFV of error-proneness at the stages of gap filling and DNA ligation will ultimately need to be borne out by in vivo analyses.

Low-Fidelity DNA Ligation in Other Systems. Our results raise the important question of whether low-fidelity DNA ligation is unique to ASFV. A candidate process in which an aberrant DNA ligase might be useful or necessary is SHM. While error-prone DNA polymerases are responsible for the generation of point mutations in SHM, the mechanistic details await clarification (*34*). Since BER and mismatch repair are likely routes for processing SHM intermediates (*34*), the generation of mismatched nicks is at least conceivable. If this is in fact the case, the protein or protein complex responsible for ligating these nicks has likely not yet been characterized since human DNA ligases I, III, and IV do not seal mismatched nicks efficiently (*20*) (B. Lamarche and M.-D. Tsai, unpublished results).

ACKNOWLEDGMENT

We thank L. K. Dixon for ASFV clones BASE and BASH and D. Parris and M. Williams for critically reading the manuscript.

REFERENCES

1. Blasco, R., Aguero, M., Almendral, J. M., and Vinuela, E. (1989) Variable and constant regions in African Swine Fever Virus DNA, *Virology 168*, 330−338.
2. Vinuela, E. (1985) African Swine Fever Virus, *Curr. Top. Microbiol. Immunol. 116*, 151−171.
3. Enjuanes, L., Cubero, I., and Vinuela, E. (1977) Sensitivity of macrophages from different species to African Swine Fever (ASF) Virus, *J. Gen. Virol. 34*, 455−463.
4. Brookes, S. M., Dixon, L. K., and Parkhouse, R. M. E. (1996) Assembly of African Swine Fever Virus: Quantitative ultrastructural analysis *in vitro* and *in vivo*, *Virology 224*, 84−92.
5. Rojo, G., Garcia-Beato, R., Vinuela, E., Salas, M. L., and Salas, J. (1999) Replication of African Swine Fever Virus DNA in infected cells, *Virology 257*, 524−536.
6. Garcia-Barreno, B., Sanz, A., Nogal, M. L., Vinuela, E., and Enjuanes, L. (1986) Monoclonal antibodies to African Swine Fever Virus: Antigenic differences among field virus isolates and viruses passaged in cell culture, *J. Virol. 58*, 385−392.
7. Dixon, L. K., and Wilkinson, P. J. (1988) Genetic diversity of African Swine Fever Virus isolates from soft ticks (*Ornithodoros moubata*) inhabiting warthog burrows in Zambia, *J. Gen. Virol. 69*, 2981−2993.
8. Yanez, R. J., Rodriguez, J. M., Nogal, M. L., Yuste, L., Enriquez, C., Rodriguez, J. F., and Vinuela, E. (1995) Analysis of the complete nucleotide sequence of African Swine Fever Virus, *Virology 208*, 249−278.
9. Showalter, A. K., and Tsai, M.-D. (2001) A DNA polymerase with specificity for five base pairs, *J. Am. Chem. Soc. 123*, 1776−1777.
10. Showalter, A. K., Byeon, I.-J. L., Su, M.-I., and Tsai, M.-D. (2001) Solution structure of a viral DNA polymerase X and evidence for a mutagenic function, *Nat. Struct. Biol. 8*, 942−946.
11. Oliveros, M., Yanez, R. J., Salas, M. L., Salas, J., Vinuela, E., and Blanco, L. (1997) Characterization of an African Swine Fever Virus 20-kDa DNA polymerase involved in DNA repair, *J. Biol. Chem. 272*, 30899−30910.
12. Tong, J., Cao, W., and Barany, F. (1999) Biochemical properties of a high fidelity DNA ligase from *Thermus* species AK16D, *Nucleic Acids Res. 27*, 788−794.
13. Dunlap, C. A., and Tsai, M.-D. (2002) Use of 2-aminopurine and tryptophan fluorescence as probes in kinetic analyses of DNA polymerase β, *Biochemistry 41*, 11226−11235.
14. Lehman, I. R. (1974) DNA ligase: Structure, mechanism, and function, *Science 186*, 790−797.
15. Odell, M., Sriskanda, V., Shuman, S., and Nikolov, D. B. (2000) Crystal structure of eukaryotic DNA ligase-adenylate illuminates the mechanism of nick sensing and strand joining, *Mol. Cell 6*, 1183−1193.
16. Magnet, S., and Blanchard, J. S. (2004) Mechanistic and kinetic study of the ATP-dependent DNA ligase of *Neisseria meningitidis*, *Biochemistry 43*, 710−717.
17. Modrich, P., and Lehman, I. R. (1973) Deoxyribonucleic acid ligase, *J. Biol. Chem. 248*, 7502−7511.
18. Lee, J. Y., Chang, C., Song, H. K., Moon, J., Yang, J. K., Kim, H.-K., Kwon, S.-T., and Suh, S. W. (2000) Crystal structure of NAD^+-dependent DNA ligase: Modular architecture and functional implications, *EMBO J. 19*, 1119−1129.
19. Pascal, J. M., O'Brien, P. J., Tomkinson, A. E., and Ellenberger, T. (2004) Human DNA ligase I completely encircles and partially unwinds nicked DNA, *Nature 432*, 473−478.
20. Bhagwat, A. S., Sanderson, R. J., and Lindahl, T. (1999) Delayed DNA joining at 3′ mismatches by human DNA ligases, *Nucleic Acids Res. 27*, 4028−4033.
21. Tomkinson, A. E., Tappe, N. J., and Friedberg, E. C. (1992) DNA ligase I from *Saccharomyces cerevisiae*: Physical and biochemical characterization of the *cdc9* gene product, *Biochemistry 31*, 11762−11771.
22. Husain, I., Tomkinson, A. E., Burkhart, W. A., Moyer, M. B., Ramos, W., Mackey, Z. B., Besterman, J. M., and Chen, J. (1995) Purification and characterization of DNA ligase III from bovine testes, *J. Biol. Chem. 270*, 9683−9690.
23. Shuman, S. (1995) *Vaccinia* virus DNA ligase: Specificity, fidelity, and inhibition, *Biochemistry 34*, 16138−16147.
24. Luo, J., Bergstrom, D. E., and Barany, F. (1996) Improving the fidelity of *Thermus thermophilus* DNA ligase, *Nucleic Acids Res. 24*, 3071−3078.
25. Liu, P., Burdzy, A., and Sowers, L. C. (2004) DNA ligases ensure fidelity by interrogating minor groove contacts, *Nucleic Acids Res. 32*, 4503−4511.
26. Mizuuchi, K., Nobbs, T. J., Halford, S. E., Adzuma, K., and Qin, J. (1999) A new method for determining the stereochemistry of DNA cleavage reactions: Application to the *Sfi*I and *Hpa*II restriction endonucleases and to the MuA transposase, *Biochemistry 38*, 4640−4648.
27. Sriskanda, V., and Shuman, S. (1998) Specificity and fidelity of strand joining by *Chlorella* virus DNA ligase, *Nucleic Acids Res. 26*, 3536−3541.
28. Lu, J., Tong, J., Feng, H., Huang, J., Alfonso, C. L., Rock, D. L., Barany, F., and Cao, W. (2004) Unique ligation properties of eukaryotic NAD^+-dependent DNA ligase from *Melanoplus sanguinipes* entomopoxvirus, *Biochim. Biophys. Acta 1701*, 37−48.
29. Sriskanda, V., and Shuman, S. (2002) Role of nucleotidyl transferase motif V in strand joining by *Chlorella* virus DNA ligase, *J. Biol. Chem. 277*, 9661−9667.
30. Wu, X., Feng, J., Komori, A., Kim, E. C., Zan, H., and Casali, P. (2003) Immunoglobulin somatic hypermutation: Double-strand DNA breaks, AID and error-prone DNA repair, *J. Clin. Immunol. 23*, 235−246.
31. Garcia-Beato, R., Salas, M. L., Vinuela, E., and Salas, J. (1992) Role of the host cell nucleus in the replication of African Swine Fever Virus DNA, *Virology 188*, 637−649.
32. Lindahl, T. (1993) Instability and decay of the primary structure of DNA, *Nature 362*, 709−715.
33. Price, A., and Lindahl, T. (1991) Enzymatic release of 5′-terminal deoxyribose phosphate residues from damaged DNA in human cells, *Biochemistry 30*, 8631−8637.
34. Li, Z., Woo, C. J., Iglesias-Ussel, M. D., Ronai, D., and Scharff, M. D. (2004) The generation of antibody diveristy through somatic hypermutation and class switch recombination, *Genes Dev. 18*, 1−11.

BI047706G